Characterisation of the Enzyme Intermediates of the Sarcoplasmic Transport ATPase by the Use of Inhibitors*

W. Boll and M. Makinose

Max-Planck-Institut für Medizinische Forschung, Abteilung Physiologie, Jahnstraße 29, 6900 Heidelberg, Bundesrepublik Deutschland

Z. Naturforsch. **38 c**, 282–289 (1983); received December 3, 1982

Sarcoplasmic Transport ATPase, Enzymes Intermediates

1. Based on a detailed reaction scheme of the phosphorylation process of the sarcoplasmic transport ATPase the inhibition mechanisms of benzoctamine, DIO 9, AMP-PNP and of Ca^{2+}-ions at relatively high concentrations (1 ~ 100 μM) were determined.

2. The inhibition mechanisms were analyzed by measuring the γ-phosphate exchange between ATP and ADP and evaluated by applying conventional and an extended Dixon plot procedures.

3. The kinetic patterns of the inhibition were shown to be compatible with the assumed reaction scheme.

4. Each inhibitor combines with definite intermediates: Benzoctamine with the intermediate species $^{Ca_2}_{Mg}E$ and $^{Ca_2}_{Mg_2}E$-ATP; AMP-PNP with $^{Ca_2}_{Mg_2}E \sim P$; DIO 9 with E and MgE and Ca^{2+} at relatively high concentrations with E.

5. The central intermediate blocked by benzoctamine can partially exist as $^{Ca_2}_{Mg_2}E\ {}^{ADP}_{P}$-benzoctamine which is detected as phosphoprotein after acid denaturation.

Introduction

The phosphoryl transfer reaction catalyzed by the Ca^{2+}-transport ATPase of the sarcoplasmic reticulum is a reversible process involving the MgATP complex and the ligand free ADP anion as substrates of the forward and backward reaction respectively [1]. Mg^{2+} and Ca^{2+}-ions are activators of the enzyme which performs transmembrane Ca^{2+} transport [2–4].

It has been demonstrated [5] that the above mentioned substrates and activators react with the enzyme in a distinct order, i.e. phosphorylation of the sarcoplasmic reticulum ATPase requires sequential activation by one Mg^{2+}-ion and two Ca^{2+}-ions [5–7] before the enzyme combines with the substrate of the forward reaction (MgATP). Regarding the backward reaction the activation by Mg^{2+} is a condition for the transfer of the enzyme's phosphoryl group to ADP. Because of its complete reversibility the activity of this reaction sequence can be measured as the exchange of γ-phosphate between ATP and ADP [4, 8].

A number of substances which inhibits the activity of the sarcoplasmic reticulum transport ATPase were identified in the past [9, 10]. Most of them, however, proved to be unsuited for the analysis of the reaction mechanism because of their relatively low inhibitory effect or of their undefined mode of inhibition. Several potent pharmacological inhibitors were revealed by a recent comprehensive screening [11]. Using some of these inhibitors (Benzoctamine, DIO 9, AMP-PNP) in this paper the sequence of the reaction steps between the sarcoplasmic transport enzyme and its activators and substrates could further be supported. Furthermore the enzyme intermediates representing the target of inhibition could be identified. A preliminary report of a part of this work has been published [12].

Materials and Methods

Preparation of sarcoplasmic reticulum

Sarcoplasmic reticulum vesicles from rabbit skeletal muscle were prepared according to Hasselbach and Makinose [13]; the protein concentration was measured by the Biuret or Kjeldahl method.

ATP-ADP Phosphate exchange activity

The compositions of the reaction mixtures are described in legends of the figures. In order to set the

---

* This work is dedicated to Prof. Adolf Butenandt, Ehrenpräsident der Max-Planck-Gesellschaft, on occasion of his 80th birthday.

Abbreviations: EGTA, ethylene glycol bis (2-aminoethylether) N,N'-tetraacetic acid; HEDTA, N-hydroxyethylethylene-diamine triacetic acid; DIO 9, 1-(2-methoxy-6-chloracridin-9-ylamino)-1-methyl-4-diethylaminobuthandihydrochloride; benzoctamine, N-methyl-9,10-ethanoanthracene-9(10H)-propanamine.

Reprint requests to Dr. M. Makinose, MPI für Medizinische Forschung, Abt. Physiologie, Jahnstr. 29, D-6900 Heidelberg, Bundesrepublik Deutschland.

0341-0382/83/0300-0282 $ 01.30/0

Dieses Werk wurde im Jahr 2013 vom Verlag Zeitschrift für Naturforschung in Zusammenarbeit mit der Max-Planck-Gesellschaft zur Förderung der Wissenschaften e.V. digitalisiert und unter folgender Lizenz veröffentlicht: Creative Commons Namensnennung-Keine Bearbeitung 3.0 Deutschland Lizenz.

This work has been digitalized and published in 2013 by Verlag Zeitschrift für Naturforschung in cooperation with the Max Planck Society for the Advancement of Science under a Creative Commons Attribution-NoDerivs 3.0 Germany License.

Zum 01.01.2015 ist eine Anpassung der Lizenzbedingungen (Entfall der Creative Commons Lizenzbedingung „Keine Bearbeitung") beabsichtigt, um eine Nachnutzung auch im Rahmen zukünftiger wissenschaftlicher Nutzungsformen zu ermöglichen.

On 01.01.2015 it is planned to change the License Conditions (the removal of the Creative Commons License condition "no derivative works"). This is to allow reuse in the area of future scientific usage.

Table I. Stability constants at pH 7.0 calculated from the constants given by Martell and Schwarzenbach [14].

	Magnesium	Calcium
ATP	3.88	3.48
ADP	3.02	2.69
EGTA	0.91	6.71
HEDTA	2.46	5.26

concentration of ionic components to desired values the amounts of the substances to be added into the reaction mixture were calculated using the stability constants listed in Table I.

In every assay the concentration of Ca-EGTA or Ca-HEDTA complexes were set at 0.5 mM so that Ca^{2+} concentration in assay was stabilized throughout the reaction time. The pH-value of the reaction mixtures containing 20 mM Histidine (pH 7.0) was readjusted immediately before the addition of sarcoplasmic reticulum vesicles.

The ATP-ADP-exchange reaction was started by addition of a mixture of [γ-^{32}P]ATP-ADP to the assay, in which the sarcoplasmic reticulum vesicles had been preincubated with the test agent for 5 min.

At desired reaction time 1 ml assay was added to 0.2 ml 0.6% Tannin-solution, and 20 µl of this mixture was transferred on a Polygram^{R}-plate (CEL 300 PEI/UV) and developed with 0.75 M KH_2PO_4 (+ 10 mM EDTA, pH 4.2). ATP- and ADP-spot were localized with UV-light, cutted out and counted in a liquid scintillation counter (Packard 3000). The amount of exchanged γ-phosphate was calculated as described previously [8].

Phosphoprotein formation

The reaction was started by addition of sarcoplasmic reticulum vesicles (0.5 mg protein/ml) and stopped after 15 sec by mixing 4 ml of the incubation medium with 16 ml of a solution containing 0.125 M perchloric acid, 1 mM unlabelled ATP and 1 mM H_3PO_4. After 15 min on ice the denaturated protein was separated by centrifugation. The pellet was washed five times with a solution (5 °C) containing 0.1 M perchloric acid and 0.2 M Na_2SO_4 and repeatedly recovered by centrifugation. The last pellet was liquefied with 1 ml Hyamine^{R} and 0.2 ml water at 60 °C and its radioactivity counted in a liquid scintillation counter.

Chemicals

ATP, ADP and AMP-PNP were purchased from Boehringer Mannheim, EGTA and HEDTA from Sigma/St. Louis and *ortho*-[^{32}P]phosphate from Amersham-Buchler/Braunschweig. DIO 9, a known inhibitor for the mitochondrial ATPase [15], was obtained from Gist Brocades nV, Delft, Netherlands. Pure Benzoctamine was a gift of Ciba-Geigy AG, Wehr/Baden. We are grateful to Dr. R. Goody, Max-Planck-Institute for Medical Research, Heidelberg for providing us with samples of AMP-PNP.

All other chemicals were in p.a. grade and acquired from Merck/Darmstadt.

Results and Discussion

Several reaction schemes for the sarcoplasmic Ca^{2+} transport ATPase were proposed based on various kinetic approaches [16–19]. Recently, the following reaction sequence has been ascertained by analysing the ATP-ADP exchange activity of the enzyme [5].

$$E \underset{K_A}{\overset{Mg^{2+}}{\rightleftharpoons}} MgE \underset{K_B}{\overset{2Ca^{2+}}{\rightleftharpoons}} \underset{Mg}{Ca_2}E \underset{K_C}{\overset{MgATP}{\rightleftharpoons}} \underset{Mg_2}{Ca_2}E\text{-ATP}$$

$$\underset{K_D}{\overset{ADP}{\rightleftharpoons}} \underset{Mg_2}{Ca_2}E \sim P \underset{K_E}{\overset{Mg^{2+}}{\rightleftharpoons}} \underset{Mg}{Ca_2}E \sim P\,. \qquad (1)$$

According to this scheme the dependence of the velocity of the γ-phosphate exchange reaction on the various reactants is given:

$$\frac{V_{max}}{V_A} = \frac{K_A K_B K_C}{[Mg][Ca]^2[MgATP]} + \frac{K_B K_C}{[Ca]^2[MgATP]} + \frac{K_C}{[MgATP]} + 1 + \frac{K_D}{[ADP]} + \frac{K_D K_E}{[ADP][Mg]} \qquad (2)$$

V_A = velocity of γ-phosphate exchange;
V_{max} = maximum exchange velocity;
$K_A - K_E$ = equilibrium constants.

It should be noticed that each term on the right side of Eq. (2) represents the relative concentrations of the respective enzyme intermediates as they appear in Eq. (1). If an inhibitor binds to an enzyme intermediate, for example MgE, and forms an inactive intermediate species MgEI, the relative size of the native (U) and of the inactivated species (UI) is given by

$$UI = I \times \frac{U}{K_I} \qquad (3)$$

where K_I is the equilibrium constant for the binding reaction of the inhibitor. Then

$$UI = I \times \frac{1}{K_I} \times \frac{K_B K_C}{[Ca]^2[MgATP]}. \quad (4)$$

Thus, in the presence of an inhibitor (I) Eq. (2) is extended by an additional term (UI).

Eq. (4) shows that, if an inhibitor blocks the enzyme species MgE, the relative size of the blocked species (UI) depends on $[Ca]^2$ and [MgATP] like (U). If another inhibitor combines with another intermediate, the relative size of the complex UI should show a different dependence on the ligand concentration. Since the factor U/K_I represents the slope of the Dixon plot (V_A^{-1} *versus* [I], Eq. (4)) the intermediate which is blocked by the inhibitor can be identified from the effect which varied ligand concentrations exert on the slope of the lines in the Dixon plot [4].

Fig. 1 a–d show the effect of benzoctamine on the ATP-ADP-exchange activity plotted according to Dixon. The slopes of these plots neither depend on the concentration of Ca^{2+} or Mg^{2+} nor on ADP yet the MgATP concentration definitely affects the slope. In Eq. (2) there is only one term which involves MgATP but not Mg^{2+}, Ca^{2+} or ADP. This term corresponds to the intermediate $^{Ca_2}_{Mg}E$ in Eq. (1). Consequently one can conclude that this species is converted into an inhibited form by binding benzoctamine. Yet it remains uncertain whether benzoctamine blocks in addition to $^{Ca_2}_{Mg}E$ its complex with MgATP, $^{Ca_2}_{Mg_2}E$-ATP. The results shown in Fig. 1 establish an essential point of the reaction sequence mentioned above (Eq. (1)), namely MgATP reacts

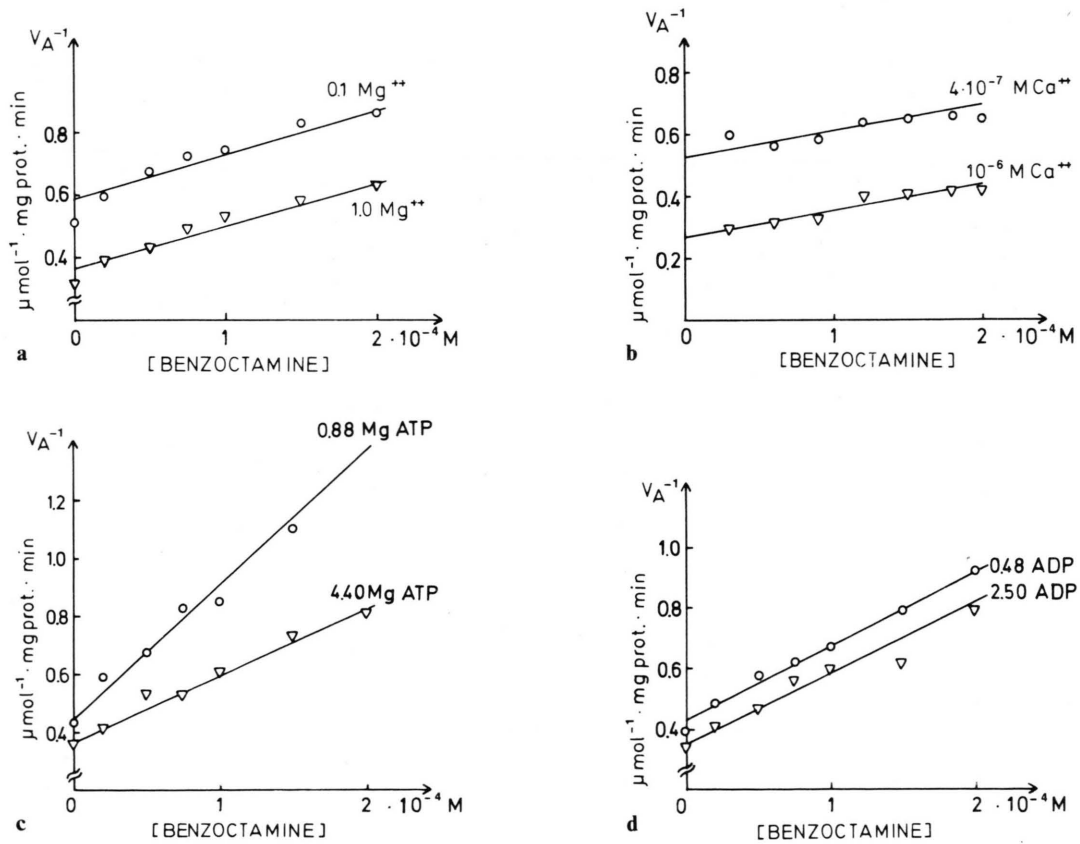

Fig. 1. Dixon-plots of the ATP-ADP-exchange activity with benzoctamine as inhibitor. Ordinate: Reciprocal rate of ATP-ADP-exchange. Abscissa: Concentration of benzoctamine. 20 mM Histidine-buffer (pH 7.0), 0.02–0.05 mg prot/ml assay, $\mu = 0.1$, 20 °C. a) With 0.1 or 1.0 mM Mg^{2+}. 3 mM MgATP, 1 mM ADP, 8 μM Ca^{2+} (EGTA-buffer). b) With 0.4 or 1.0 μM Ca^{2+} (HEDTA-buffer). 3 mM MgATP, 1 mM ADP, 0.5 mM Mg^{2+}. c) With 0.88 or 4.4 mM MgATP. 1 mM ADP, 1 mM Mg^{2+}, 8 μM Ca^{2+} (EGTA-buffer). d) With 0.48 or 2.5 mM ADP. 1.76 mM MgATP, 1 mM Mg^{2+}, 8 μM Ca^{2+} (EGTA-buffer).

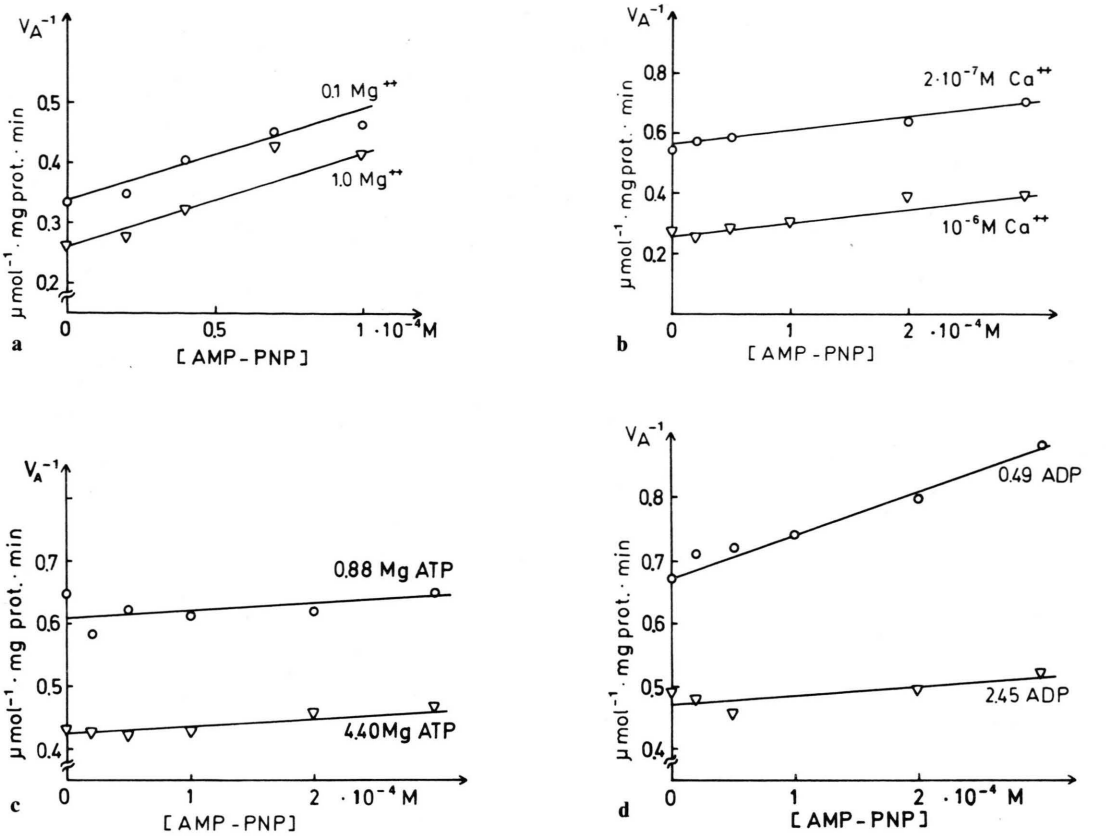

Fig. 2. Dixon-plots of the ATP-ADP-exchange activity with AMP-PNP as inhibitor. Ordinate: Reciprocal rate of ATP-ADP-exchange. Abscissa: Concentration of AMP-PNP. 20 mM Histidine-buffer (pH 7.0), 0.02–0.05 mg prot/ml assay, $\mu = 0.1$, 20 °C. a) With 0.1 or 1.0 mM Mg^{2+}. 1.5 mM MgATP, 0.5 mM ADP, 1 μM Ca^{2+} (EGTA-buffer). b) With 0.2 or 1.0 μM Ca^{2+}. 1.5 mM MgATP, 0.3 mM ADP, 0.5 mM Mg^{2+}. c) With 0.88 or 4.4 mM MgATP, 1 mM ADP, 1 mM Mg^{2+}, 8 μM Ca^{2+} (EGTA-buffer). d) With 0.49 or 2.45 mM ADP. 1.77 mM MgATP, 1 mM Mg^{2+}, 8 μM Ca^{2+} (EGTA-buffer).

with the enzyme after the binding of Mg^{2+} and Ca^{2+} to the enzyme.

In the presence of the inhibitor AMP-PNP the slope of the Dixon plot of the ATP-ADP-exchange activity shows no dependence on Ca^{2+} or Mg^{2+} concentration as observed with benzoctamine. Although AMP-PNP is considered to be an ATP-analogue the slope of the Dixon plot depends on the ADP concentration but not on the MgATP concentration (Fig. 2c, d) indicating that this inhibitor blocks $^{Ca_2}_{Mg_2}E \sim P$. Again it is impossible to exclude an additional inhibition of the central intermediate $^{Ca_2}_{Mg_2}E$-ATP by AMP-PNP.

The described ambiguity can be resolved by plotting the values $V_A^{-1} \times$ [MgATP] (in the case of benzoctamine) or $V_A^{-1} \times$ [ADP] (in the case of AMP-PNP) *versus* the inhibitor concentration ([*I*]) (Fig. 3a, b). If the central complex ($^{Ca_2}_{Mg_2}E$-ATP) of the reaction and the species $^{Ca_2}_{Mg}E$ were both blocked by benzoctamine the slope (q) of this plot can be formulated as follows:

$$q = \left(\frac{K_C}{K_I} + \frac{[\text{MgATP}]}{K_I'}\right)\frac{1}{V_{max}} \tag{5}$$

where K_I' is the equilibrium constant of the inhibitor's reaction with the central complex. In other words the slope of this plot should depend positively on [MgATP]. Fig. 3a shows that this indeed is the case. If benzoctamine did not block the central complex but only the $^{Ca_2}_{Mg}E$ complex,

$$q = \frac{K_C}{K_I} \cdot \frac{1}{V_{max}} \tag{6}$$

q should be independent of [MgATP] and constant.

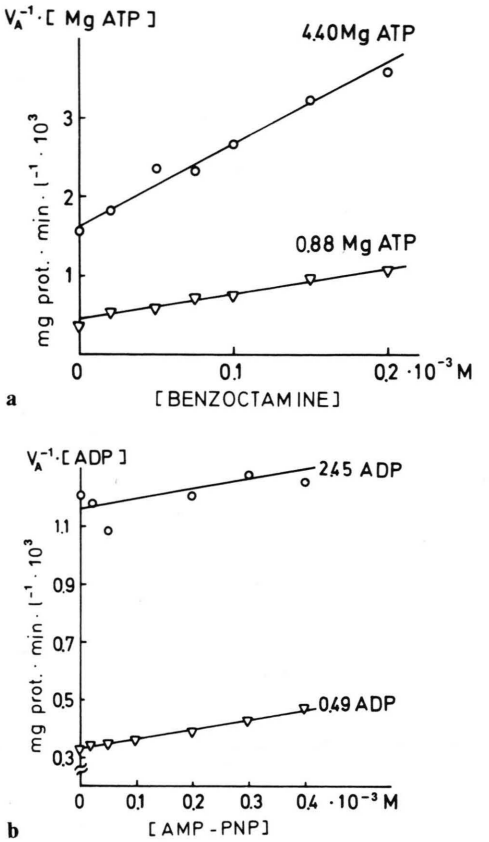

Fig. 3. Combined Dixon Hanes-Woolf-plots ($V_A^{-1} \times$[MgATP] *versus* inhibitor concentration. a) Replotting of Fig. 1c. b) Replotting of Fig. 2d.

Regarding AMP-PNP the same procedure can be applied (Fig. 3b). Since the slope of this plot is independent of the ADP concentration one must assume that AMP-PNP solely binds to the intermediate $^{Ca_2}_{Mg_2}E \sim P$, presumably in competition with ADP.

Fig. 4a and b show that the level of phosphoprotein formation of the sarcoplasmic reticulum transport ATPase is increased by the addition of either benzoctamine or AMP-PNP. Since benzoctamine binds to the central complex (Fig. 3a) one has to conclude that this intermediate presumably includes a phosphorylated enzyme species of the transport ATPase protein. Dieterle [21] has suggested that in acetyl phosphate containing assays a ternary phosphoprotein complex is formed after addition of ADP and AMP-PNP. Similarly, Nakamura *et al.* [22] infered from kinetic data of pNPP-splitting the presence of a *p*-nitrophenol binding phosphoprotein. Presumably the central complex in Eq. (1) involves an ADP-binding intermediate ($^{Ca_2}_{Mg_2}E \prec^{ADP}_{P}$) which is detectable as phosphoenzyme together with other phosphorylated species. If AMP-PNP binds to $^{Ca_2}_{Mg_2}E \sim P$ competing with ADP for the same binding site the consecutive formation of the $^{Ca_2}_{Mg_2}E \prec^{AMP\text{-}PNP}_{P}$ intermediate should lead to the increase of phosphoprotein formation observed (Fig. 4b).

Using DIO 9 as inhibitor the slopes of the Dixon plots become steeper when the concentrations of Mg^{2+}, Ca^{2+} or MgATP are reduced [12].

In contrast the slopes proved to be independent of the ADP concentration. This means that the ADP

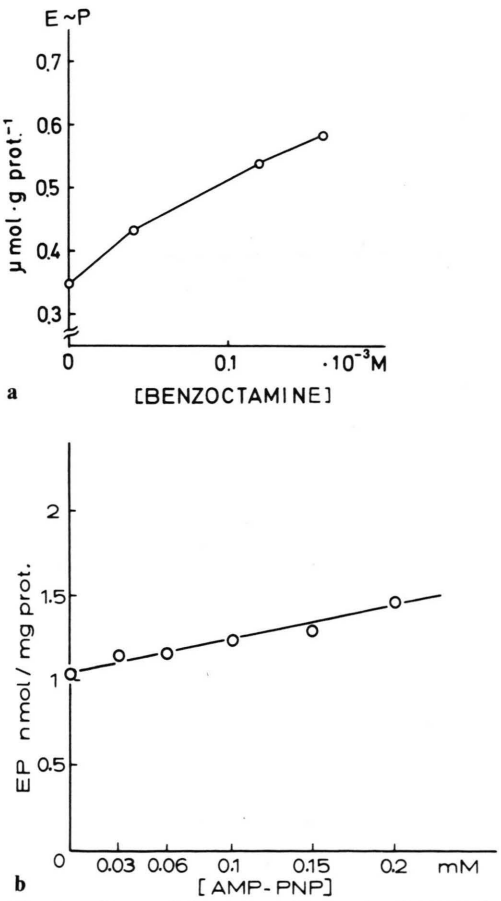

Fig. 4. Effect of benzoctamine and AMP-PNP on the phosphoprotein formation in assays containing ADP. Ordinate: Phosphoprotein formation. Abscissa: Concentration of inhibitor. 20 mM Histidine-buffer (pH 7.0), 0.5 mg prot/ml assay, $\mu = 0.1$, 0 °C. a) With benzoctamine. 1 mM MgATP, 1 mM ADP, 0.5 mM Mg^{2+}, 0.4 µM Ca^{2+}. b) With AMP-PNP. 3 mM MgATP, 1 mM ADP, 0.1 mM Mg^{2+}, 8 µM Ca^{2+}.

free phosphorylated intermediates do not combine with DIO 9. From the primary Dixon plots, however, it is impossible to localize the enzyme target of DIO 9 inhibition. In order to obtain detailed information the Dixon procedure was extended.

A number of experiments was carried out varying the concentrations of DIO 9 and of a certain ligand. The intercept on the abscissa (p) of the primary plots according to Dixon were determined and subsequently replotted against the corresponding ligand concentration. The p value depends on ligand concentrations ([L]) and on the equilibrium constants between ligands and inhibitors of the corresponding enzyme species but is independent of the inhibitor concentration (see Eq. (6)). From the behaviour of the p value when the concentration of a certain ligand is varied one can specify the blocked intermediate. Figure 5 shows all possible patterns of plotting p *versus* [L] and comments on the corresponding inhibition mechanism.

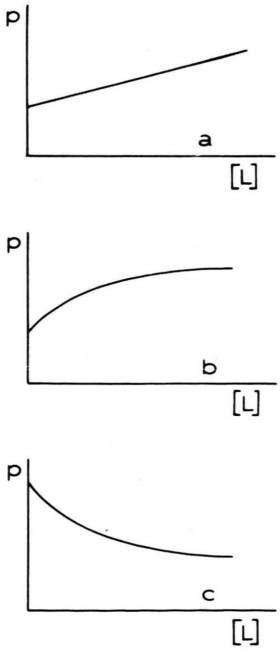

Fig. 5. Schematic pattern of the new plotting procedure (p *versus* ligand concentration [L]) for inhibition analysis. a) Ascending straight line: The relative size of all intermediates which the inhibitor interact depends on [L]. b) Ascending curve: At least two intermediate species are blocked by the inhibitor. The target intermediates *must* involve at least one [L] dependent and one [L] independent species. c) Descending curve: The intermediates, the relative sizes of which depend on [L], are not the target of the inhibitor.

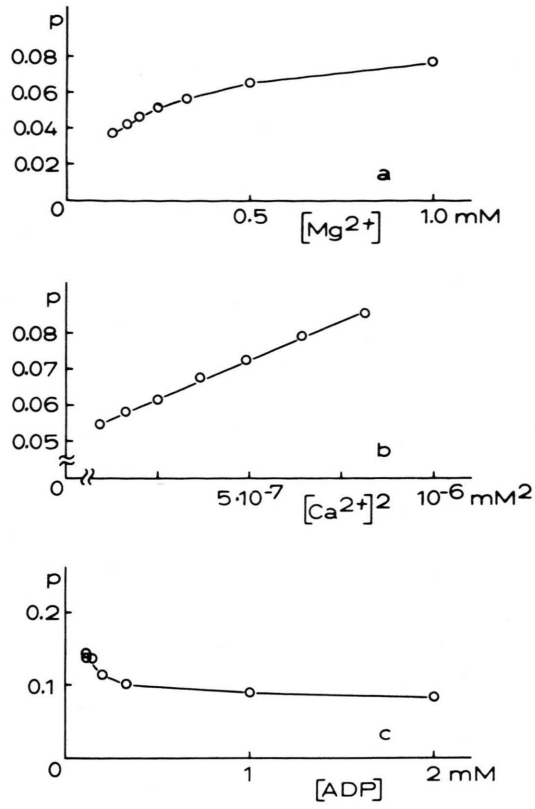

Fig. 6. Analysis of DIO 9 inhibition by specific plotting (see text). A number of Dixon plots of the exchange rate (inhibitor DIO 9, 0.02–0.2 mM) was carried out in varying ligand concentrations. The abscissa intersection (p) of each Dixon plot was replotted against the corresponding ligand concentration. 20 mM Histidine-buffer (pH 7.0), 0.02–0.05 mg prot/ml assay, $\mu = 0.1$, 20 °C. a) Varied ligand Mg^{2+} (0.125–1 mM). 3 mM MgATP, 1 mM ADP, 0.4 μM Ca^{2+} (EGTA-buffer). b) Varied ligand Ca^{2+} (0.3–0.9 μM HEDTA-buffer). 3 mM ATP, 1 mM ADP, 0.5 mM Mg^{2+}. c) Varied ligand ADP (0.1–2 mM). 2 mM MgATP, 0.5 mM Mg^{2+}, 0.4 μM Ca^{2+} (EGTA-buffer).

The analysis of DIO 9 inhibition on the ADP-ATP-exchange activity is presented in Fig. 6. The p value shows a non-linear increase *versus* Mg^{2+} concentration, a linear increase versus the square of Ca^{2+} concentration (as mentioned in the introduction, the controlled variable should be the square of [Ca^{2+}] since the sarcoplasmic reticulum transport enzyme is activated by two Ca^{2+} ions) and a non-linear decrease versus ADP concentration. According to the possibility described in Fig. 5 one must conclude that DIO 9 interacts with the enzyme species E and MgE (Eq. (1)).

Hence the p value is given by:

$$p = \frac{K_A K_I K_I'}{(K_A K_I' + K_I[Mg])} + \frac{[Mg] K_I K_I'}{(K_A K_I' + K_I[Mg])} + \frac{[Mg][Ca]^2 K_I K_I'}{(K_A K_B K_I' + K_B K_I[Mg])} + \frac{[Mg][Ca]^2[MgATP] K_I K_I'}{(K_A K_B K_C K_I' + K_B K_C K_I[Mg])} + \frac{K_D[Mg][Ca]^2[MgATP] K_I K_I'}{[ADP](K_A K_B K_C K_I' + K_B K_C K_I[Mg])}. \quad (6)$$

Eq. (6) fulfills the feature of the curves appearing in Fig. 6a–c. None of the equations of the p value derived from another version of inhibition mechanism can meet the observed pattern (Fig. 6a–c). The results of Fig. 6 conversely establish another essential point in the reaction sequence (Eq. (1)), namely that Mg^{2+} ions bind to the enzyme before the enzyme is activated by Ca^{2+}-binding. The inverse binding sequence of Mg^{2+}- and Ca^{2+}-ions does not result in the pattern of Fig. 6a and b.

It is well known that the ATP-splitting of the sarcoplasmic reticulum enzyme is inhibited if the Ca^{2+} concentration is raised above the optimum concentration [23–26]. The rate of ATP-ADP-exchange is also inhibited at relatively high Ca^{2+} concentrations [27] and the inhibition range depends on the Mg^{2+} concentration in the assay (Fig. 7).

Fig. 8a, b shows the results of the analysis of the inhibitory effect of Ca^{2+} on the ATP-ADP-exchange rate. The p value exhibits linear increase *versus* Mg^{2+} concentration and non-linear decrease *versus* ADP concentration. According to the predictions illustrated in Fig. 5 Ca^{2+} at high concentrations binds exclusively to the ligand free enzyme species (E in Eq. (1)) apparently in competition with Mg^{2+} ions.

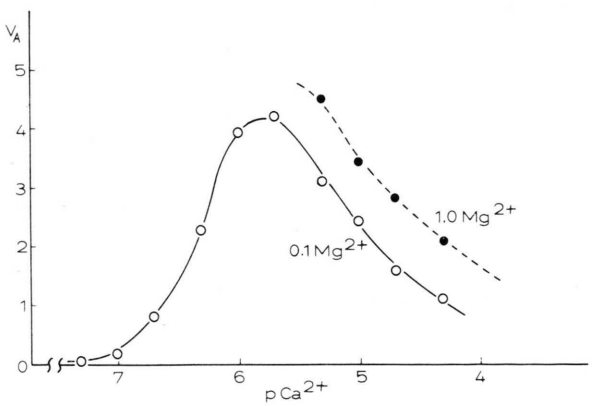

Fig. 7. Activation and inhibition of ATP-ADP-exchange activity by Ca^{2+} ions. Ordinate: The rate of ATP-ADP-exchange in µmol P/mg prot · min. 20 mM Histidine-buffer (pH 7.0), 0.02 mg prot/ml assay, 1 mM MgATP, 0.5 mM ADP, 0.5 mM Ca-HEDTA, $\mu = 0.1$, 20 °C.

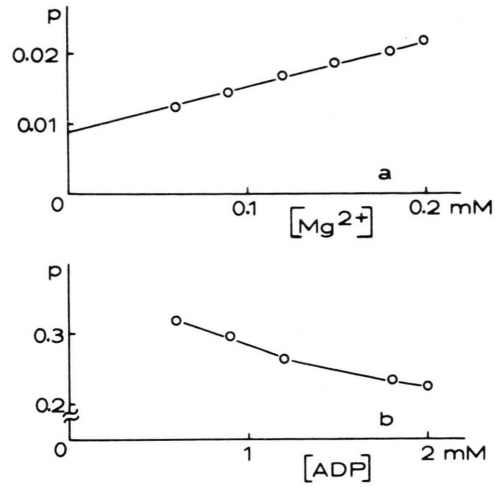

Fig. 8. Analysis of Ca^{2+} inhibition by specific plotting. The analysing procedure was carried out in the same way as in Fig. 6 in the presence of relatively high concentration of Ca^{2+} (0.8–20 µM) instead of DIO 9. 20 mM Histidine-buffer (pH 7.0). 0.02–0.05 mg prot/ml assay, $\mu = 0.1$, 20 °C. a) Varied ligand Mg^{2+} (0.06–0.2 mM). 3 mM MgATP, 1 mM ADP, HEDTA-buffer. b) Varied ligand ADP (0.6–2.0 mM). 3 mM MgATP, 0.2 mM Mg^{2+}.

In contrast to the conventional Dixon plots the new plotting method furnishes all necessary information that is needed to localize the target intermediate. Furthermore the criterion of this method is the shape of the graph which is in general much easier to judge objectively than parallelity of two or more straight lines.

From the experimental data used for Fig. 8a, the Hill coefficient of Ca^{2+} binding to the Mg^{2+} activation site was calculated and amounts to 0.97 ± 0.07. It means that one Ca^{2+} ion is needed to expel Mg^{2+} from its binding site.

From kinetic investigations of the transport ATPase activity Vianna [7] described Mg^{2+} to be a Ca^{2+} competitor and pointed out the mutual dependence of the optimum concentrations of Ca^{2+} and Mg^{2+} within the activating concentration range of ATP-splitting. The competition between Ca^{2+} and Mg^{2+} ions described here (Fig. 8) does not take place at the high affinity Ca^{2+} binding site of the

enzyme discussed by Vianna but at the Mg^{2+} binding site. Thus, the replacement of Mg^{2+} ions by Ca^{2+} ions causes an inhibition of the phosphorylation of the enzyme.

Dupont [28] has suggested a conversion of a magnesium-phosphoenzyme [(2Ca) · E · Mg · P] to a calcium-phosphoenzyme [(2Ca) · E · Ca · P] which is also ADP sensitive. The result of the Fig. 8 does not absolutely exclude this possibility. However, it indicates clearly that the exchange between Ca^{2+} and Mg^{2+} ions at the Mg^{2+} binding site mainly takes place via the ligand free intermediate while the Ca^{2+}-Mg^{2+}-exchange on the other intermediate can be neglected.

[1] M. Makinose and W. Boll in: Cation Flux Across Biomembranes (Y. Mukohata et al., Eds.), p.89, Academic Press, Calif. 1979.
[2] W. Hasselbach and M. Makinose, Biochem. Z. **333,** 518 (1961).
[3] S. Ebashi and F. Lippmann, J. Cell. Biol. **14,** 389 (1962).
[4] W. Hasselbach and M. Makinose, Biochem. Biophys. Res. Commun. **7,** 132 (1962).
[5] W. Boll, Dr. med. Thesis, Universität Heidelberg (1982) in preparation for publication.
[6] R. The and W. Hasselbach, Eur. J. Biochem. **28,** 357 (1972).
[7] A. L. Vianna, Biochim. Biophys. Acta **410,** 389 (1975).
[8] M. Makinose, Eur. J. Biochem. **10,** 74 (1969).
[9] H. Balzer, M. Makinose, and W. Hasselbach, Naunyn-Schmiedbergs Arch. Pharmak. Exp. Path. **260,** 444 (1968).
[10] D. Temple, M. Makinose, and W. Hasselbach, Naunyn-Schmiedbergs Arch. **282,** 187 (1974).
[11] G. Loer, Dr. med. Thesis, Universität Heidelberg (1982) in preparation for publication.
[12] M. Makinose and W. Boll in: Function and Molecular Aspects of Biomembrane Transport (E. Quagliariello et al., Eds.), p. 115, Elsevier/North Holland Biomedical Press 1979.
[13] W. Hasselbach and M. Makinose, Biochem. Z. **339,** 94 (1963).
[14] A. E. Martell and G. Schwarzenbach, Helv. Chim. Acta **39,** 653 (1956).
[15] R. J. Guillory, Biochim. Biophys. Acta **89,** 197 (1964).
[16] W. Hasselbach, Biochim. Biophys. Acta **515,** 23 (1978).
[17] M. Makinose, Calcium Binding Proteins (W. Drabikowski et al., Eds), p. 507, Elsevier Scientific Publishing Co., Amsterdam 1974.
[18] L. de Meis, The Sarcoplasmic Reticulum, John Wiley & Sons, New York 1981.
[19] T. Yamamoto et al., Current Topics in Bioenergetics (D. R. Sanadi, Ed.), **vol. 9,** p. 179, Academic Press, Calif. 1979.
[20] M. Dixon, Biochem. J. **55,** 170 (1953).
[21] F. Dieterle, Dr. med. Thesis, Universität Heidelberg 1980.
[22] Y. Nakamura and Y. Tonomura, J. Biochem. **83,** 571 (1978).
[23] W. Hasselbach, Progr. Biophys. Chem. **14,** 167 (1964).
[24] G. Inesi, E. Maring, A. J. Murphy, and B. H. McFarland, Arch. Biochem. Biophys. **138,** 285 (1974).
[25] A. Martonosi and R. Feretos, J. Biol. Chem. **239,** 659 (1964).
[26] S. Yamada and Y. Tonomura, J. Biochem. **72,** 417 (1972).
[27] N. Ronzani, A. Migala, and W. Hasselbach, Eur. J. Biochem. **101,** 593 (1979).
[28] Y. Dupont, Eur. J. Biochem. **109,** 231 (1980).